Approach for noncollinear GGA kernels in closed-shell systems

Zhichen Pu, Ning Zhang, Hong Jiang, and Yunlong Xiao*
College of Chemistry and Molecular Engineering, Peking University, Beijing 100871, People's Republic of China

(Received 28 September 2021; revised 21 December 2021; accepted 22 December 2021; published 10 January 2022)

Exchange-correlation kernels in density functional theory are the second-order derivatives of the exchange-correlation functionals with respect to the density matrix. For collinear functionals, the forms of kernels are well known, and their applications in calculating responses of electrons to predict properties of molecules and materials are mature. However, kernels of noncollinear functionals in closed-shell systems, except for LDA (local density approximation), are generally unknown, at least mathematically ill-defined, suffering from the indeterminate forms of 0 divided by 0. We find that such singularities in noncollinear GGA (generalized gradient approximation) kernels can be removed by introducing a proper limit process and approaching the limit after the calculations of derivatives have been done. Following this idea, mathematically well-defined noncollinear GGA kernels for closed-shell systems emerge naturally. Theoretically, these kernels are shown to be numerically stable and spin-rotational symmetry preserved. Numerical tests on excitation energies and spectroscopy parameters present reasonable results, indicating the applicability of this methodology.

DOI: 10.1103/PhysRevB.105.035114

I. INTRODUCTION

Density functional theory (DFT), due to its opportune balance between accuracy and efficiency, has become the most popular method in calculating electronic structures of molecules and materials. To treat spin polarization properly, DFT has been extended to spin-density functional theory (SDFT) [1,2]. Presently, the most commonly used spin functionals are collinear functionals

$$E_{\rm xc}^{\rm col} = E_{\rm xc}^{\rm col}[n_\uparrow(\boldsymbol{r}), n_\downarrow(\boldsymbol{r})], \tag{1}$$

where $n_\uparrow$ and $n_\downarrow$ are the so-called "up(α)" and "down(β)" spin densities, respectively. The exchange-correlation energy functionals (1) can also be expressed in terms of density $n = n_\uparrow + n_\downarrow$ and spin-density $s = n_\uparrow - n_\downarrow$, i.e.,

$$E_{\rm xc}^{\rm col} = E_{\rm xc}^{\rm col}[n(\boldsymbol{r}), s(\boldsymbol{r})], \tag{2}$$

and the spin-density s of a system is evaluated as the z component of the spin magnetization vector $\boldsymbol{m}(\boldsymbol{r})$

$$s(\boldsymbol{r}) = m_z(\boldsymbol{r}). \tag{3}$$

The adoption of Eq. (3) hints that collinear functionals can only treat collinear spin systems properly, where $\boldsymbol{m}(\boldsymbol{r})$ at different spatial grids $\boldsymbol{r}$ is parallel to the same line without loss of generality defined along the z axis.

Noncollinear spin systems, where the directions of $\boldsymbol{m}$ everywhere generally do not align on the same line, are common in magnetic materials and systems significantly affected by spin-orbit couplings. To describe noncollinear spin systems, noncollinear SDFT

$$E_{\rm xc}^{\rm NC} = E_{\rm xc}^{\rm NC}[n(\boldsymbol{r}), \boldsymbol{m}(\boldsymbol{r})], \tag{4}$$

instead of collinear SDFT (2) should be used. Due to the difficulties of developing noncollinear functionals from the very beginning, it is more practical to extend collinear functionals to their noncollinear counterparts. In 1998, Kübler *et al.* proposed an approach to realize the extension [3],

$$E_{\rm xc}^{\rm NC} = E_{\rm xc}^{\rm col}[n(\boldsymbol{r}), s(\boldsymbol{r}) = |\boldsymbol{m}(\boldsymbol{r})|], \tag{5}$$

in which only the length of $\boldsymbol{m}$ is adopted to evaluate the value of noncollinear functional for the purpose of maintaining the invariance of rotation in spin space. The kernel of noncollinear LDA (local density approximation) [4] functional based on Eq. (5) has achieved great success in predicting excitation energies [5] and magnetic properties [6]. Unfortunately, kernels of noncollinear GGA (generalized gradient approximation) [7,8] functionals

$$E_{\rm xc}^{\rm NC} = \int f(n(\boldsymbol{r}), \nabla n(\boldsymbol{r}), s(\boldsymbol{r}), \nabla s(\boldsymbol{r}))\mathrm{d}\boldsymbol{r}, \tag{6}$$

based on Eq. (5), suffer from numerical problems for both open-shell and closed-shell systems. Comprehensive discussions of noncollinear GGA kernels can be found in Ref. [9], where it is claimed that *this (numerical instability) holds for all noncollinear ansatzes discussed in this work since they all incorporate, in one way or another, a square-root function*, indicating that it is an unrealistic task to derive stable noncollinear GGA kernels, strictly following the definition of noncollinear SDFT. We cautiously analyze the mathematically ill-defined terms in noncollinear GGA kernels for closed-shell systems and propose the infinitesimal sphere limit (ISL) approach to calculate the noncollinear GGA kernels. Basically, a limit process, $\boldsymbol{m} \to \boldsymbol{0}$, is introduced in the ISL approach, and $\boldsymbol{m}$ approaches the zero vector only after the calculations of derivatives of functionals with respect to the density matrix. In Section II, ISL will be compared with two approaches, which also treat noncollinear GGA kernels for

*xiaoyl@pku.edu.cn

closed-shell systems, one proposed by Bast and co-workers [10] and another by Egidi and co-workers [11].

II. THEORY

Exchange-correlation energy (4) is a functional of density $n(\boldsymbol{r})$ and spin magnetization vector $\boldsymbol{m}(\boldsymbol{r})$, also a function of the density-matrix $\boldsymbol{D}$. To calculate responses of systems to perturbations, derivatives of the exchange-correlation energy with respect to the density matrix need to be calculated.

The matrix element of the noncollinear GGA exchange-correlation potential $V^{\rm xc}$ for closed-shell systems is the first-order derivative of $E_{\rm xc}$ with respect to the element of density-matrix $\boldsymbol{D}$ (responses of closed-shell systems generally involve nonvanishing spin density, which explains why SDFT is needed),

$$V^{\rm xc}_{pq} = \frac{\partial E_{\rm xc}}{\partial D_{qp}} = \int \frac{\partial f}{\partial \gamma_i}\frac{\partial \gamma_i}{\partial D_{qp}}{\rm d}\boldsymbol{r}, \tag{7}$$

where p, q are indexes of the one-electron basis set, and $\gamma_i (i = 1, 2, \ldots, 8)$ stands for n, $\nabla_x n$, $\nabla_y n$, $\nabla_z n$, s, $\nabla_x s$, $\nabla_y s$, $\nabla_z s$, respectively. The Einstein summation convention over repeated indexes is always used. Equation (7) involves $\frac{\partial s}{\partial D_{qp}} = \frac{\boldsymbol{m}}{s}\cdot\frac{\partial \boldsymbol{m}}{\partial D_{qp}}$, which has the possibility of triggering $\frac{0}{0}$ singularities, and also $\frac{\partial \nabla s}{\partial D_{qp}}$. Thanks to the time-reversal symmetry for closed-shell systems, the latent $\frac{0}{0}$ singular term vanishes and has no contribution to exchange-correlation potential.

However, the singularities in the noncollinear GGA kernel, the second-order derivative of $E_{\rm xc}$, cannot be eliminated by time-reversal symmetry. The noncollinear GGA kernel for closed-shell systems reads

$$K_{pqrs} = \int \frac{\partial^2 f}{\partial D_{qp}\partial D_{rs}}{\rm d}\boldsymbol{r}, \tag{8}$$

which can be divided into three terms,

$$K_{pqrs} = K^{\rm nn}_{pqrs} + K^{\rm ns}_{pqrs} + K^{\rm ss}_{pqrs}. \tag{9}$$

The first term in Eq. (9), $K^{\rm nn}_{pqrs} = \sum_{i=1}^{4}\sum_{j=1}^{4}\int \frac{\partial^2 f}{\partial\gamma_i\partial\gamma_j}\frac{\partial\gamma_i}{\partial D_{qp}}\frac{\partial\gamma_j}{\partial D_{rs}}{\rm d}\boldsymbol{r}$, is spin independent and numerically stable. The second term in Eq. (9), $K^{\rm ns}_{pqrs} = (\sum_{i=1}^{4}\sum_{j=5}^{8} + \sum_{i=5}^{8}\sum_{j=1}^{4})\int \frac{\partial^2 f}{\partial\gamma_i\partial\gamma_j}\frac{\partial\gamma_i}{\partial D_{qp}}\frac{\partial\gamma_j}{\partial D_{rs}}{\rm d}\boldsymbol{r}$, vanishes due to time-reversal symmetry in closed-shell systems. Singularities of the noncollinear GGA kernel only exist in $K^{\rm ss}_{pqrs}$, the third term of Eq. (9),

$$\begin{aligned} K^{\rm ss}_{pqrs} &= \sum_{i=5}^{8}\sum_{j=5}^{8}\int \frac{\partial^2 f}{\partial\gamma_i\partial\gamma_j}\frac{\partial\gamma_i}{\partial D_{qp}}\frac{\partial\gamma_j}{\partial D_{rs}}{\rm d}\boldsymbol{r} \\ &\quad + \sum_{i=5}^{8}\int \frac{\partial f}{\partial\gamma_i}\frac{\partial^2\gamma_i}{\partial D_{qp}\partial D_{rs}}{\rm d}\boldsymbol{r} \\ &= \sum_{i=5}^{8}\sum_{j=5}^{8}\int \frac{\partial^2 f}{\partial\gamma_i\partial\gamma_j}\frac{\partial\gamma_i}{\partial D_{qp}}\frac{\partial\gamma_j}{\partial D_{rs}}{\rm d}\boldsymbol{r} \\ &\quad + \sum_{i=5}^{8}\sum_{j=5}^{8}\int \frac{\partial^2 f}{\partial\gamma_i\partial\gamma_j}\gamma_j\frac{\partial^2\gamma_i}{\partial D_{qp}\partial D_{rs}}{\rm d}\boldsymbol{r}, \end{aligned} \tag{10}$$

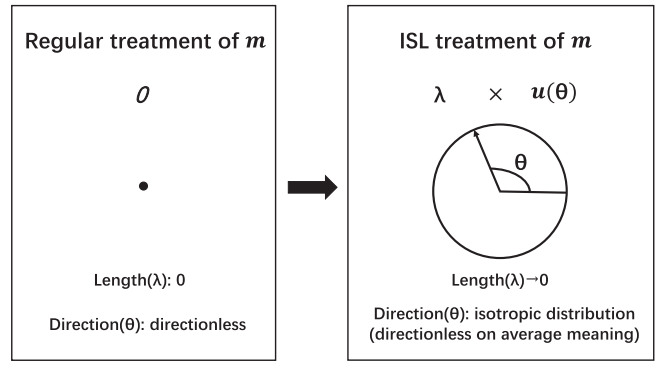

FIG. 1. ISL treatment in a two-dimensional system; due to the time-reversal symmetry, magnetization vector $\boldsymbol{m}$ is $\boldsymbol{0}$ everywhere for closed-shell systems. A regular treatment of the response on $\boldsymbol{0}$ is singular. In ISL, $\boldsymbol{m}$ is represented by a set of vectors $\lambda\boldsymbol{u}(\Omega)$ (for a two-dimensional system, Ω is the polar angle θ; for a three-dimensional system, Ω is the solid angle with parameters (θ, ϕ) in spherical coordinates), with length controlled by λ, approaching zero in the end, and direction controlled by $\boldsymbol{u}$ in an isotropic distribution.

which can be further divided into three terms,

$$K^{\rm ss}_{pqrs} = K^{\rm LDA}_{pqrs} + K^{\rm mix}_{pqrs} + K^{\rm grd}_{pqrs}. \tag{11}$$

The first term of Eq. (11), $K^{\rm LDA}_{pqrs} = \int \frac{\partial^2 f}{\partial s^2}\frac{\partial \boldsymbol{m}}{\partial D_{qp}}\cdot\frac{\partial \boldsymbol{m}}{\partial D_{rs}}{\rm d}\boldsymbol{r}$ is the pure spin contribution, which is numerically stable and shares the same form as its LDA counterpart [5]. The second term of Eq. (11), $K^{\rm mix}_{pqrs} = \int \frac{\partial^2 f}{\partial s\partial\nabla s}\cdot\nabla(\frac{\partial \boldsymbol{m}}{\partial D_{qp}}\cdot\frac{\partial \boldsymbol{m}}{\partial D_{rs}}){\rm d}\boldsymbol{r}$, describes a mixed second-order response from spin and its gradient, which is also numerically stable. The last term of Eq. (11), the pure gradient contribution,

$$K^{\rm grd}_{pqrs} = \int \frac{1}{2}\frac{\partial^2 f}{\partial\nabla_\alpha s\partial\nabla_\beta s}\left(\frac{\partial^2[(\nabla_\alpha s)(\nabla_\beta s)]}{\partial D_{qp}\partial D_{rs}}\right){\rm d}\boldsymbol{r}, \tag{12}$$

with the Greek alphabet for x, y, z, is the only singular term in the noncollinear GGA kernel owing to the $\frac{0}{0}$ indeterminate forms inside parentheses analogous to noncollinear GGA potential but unable to be removed by time-reversal symmetry. The $\frac{0}{0}$ indeterminate forms can only be evaluated in a limit process, $\boldsymbol{m}(\boldsymbol{r}) \to \boldsymbol{0}$ in this specific problem. However, when the function $\boldsymbol{m}(\boldsymbol{r})$ goes to zero vector, different limit processes generally provide different results. A sensible limit process should be avoiding singularities, preserving spin-rotation symmetry, and simple. Based on these guidelines, the ISL approach is proposed and outlined below.

First, for any vector $\boldsymbol{m}$, its proximity vector $\boldsymbol{m}(\lambda, \Omega)$ is introduced,

$$\boldsymbol{m}(\lambda, \Omega) = \boldsymbol{m} + \lambda\boldsymbol{u}(\Omega), \tag{13}$$

where λ is a small real number to indicate how close $\boldsymbol{m}$ and $\boldsymbol{m}(\lambda, \Omega)$ are, and $\boldsymbol{u}(\Omega)$ is a unit vector directing to the orientation described by solid-angle Ω. For closed-shell systems, $\boldsymbol{m}(\lambda, \Omega)$ reads

$$\boldsymbol{m}(\lambda, \Omega) = \lambda\boldsymbol{u}(\Omega), \tag{14}$$

as depicted in Fig. 1. With note $\langle\cdots\rangle_\Omega$ to be the average over all directions Ω, it is evident that

$$\boldsymbol{m} = \lim_{\lambda\to 0}\langle \boldsymbol{m}(\lambda,\Omega)\rangle_\Omega. \tag{15}$$

Actually, two stronger conditions, $\boldsymbol{m} = \langle \boldsymbol{m}(\lambda,\Omega)\rangle_\Omega$ and $\boldsymbol{m} = \lim_{\lambda\to 0}\boldsymbol{m}(\lambda,\Omega)$, hold. Regular treatment of noncollinear GGA reads

$$O = O[\boldsymbol{m}] = O\Big[\lim_{\lambda\to 0}\langle \boldsymbol{m}(\lambda,\Omega)\rangle_\Omega\Big], \tag{16}$$

through the proximity vector, with $O[\cdots]$ denoting an expression depending on derivatives of the exchange-correlation functional with respect to the density matrix, which is still a functional of $\boldsymbol{m}(\boldsymbol{r})$. In Eq. (16), the regular treatment, λ approaches zero before the calculations of derivatives. Instead of Eq. (16), in ISL approach, λ approaches zero after the calculations of derivatives in O,

$$O^{\mathrm{ISL}}[\boldsymbol{m}] = \lim_{\lambda\to 0}\langle O[\boldsymbol{m}(\lambda,\Omega)]\rangle_\Omega, \tag{17}$$

which becomes

$$K^{\mathrm{ISL}} = \lim_{\lambda\to 0}\langle K[\boldsymbol{m}(\lambda,\Omega)]\rangle_\Omega, \tag{18}$$

when the kernel is concerned.

The noncollinear kernel in the ISL approach (18) is formally calculated as follows: (1) Replace $\boldsymbol{m}$ by its proximity vector $\boldsymbol{m}(\lambda,\Omega)$, as described in Eq.(13); (2) calculate $s(\lambda,\Omega) = |\boldsymbol{m}(\lambda,\Omega)|$ and its derivatives with respect to $\boldsymbol{D}$, $(\nabla s)(\lambda,\Omega) = \nabla(s(\lambda,\Omega))$ and its derivatives with respect to $\boldsymbol{D}$, and the kernel $K[\boldsymbol{m}(\lambda,\Omega)]$; (3) calculate K^{ISL} according to Eq. (18).

In our program, the limit process described in Eq. (18) is realized analytically instead of numerically. The numerically stable K^{nn}_{pqrs} and K^{ns}_{pqrs} in Eq. (9), K^{LDA}_{pqrs} and K^{mix}_{pqrs} of K^{ss}_{pqrs} in Eq.(11) remain in their original forms unchanged in ISL treatment (18), but the numerically singular term K^{grd}_{pqrs} (12) becomes numerically stable in ISL, reading

$$K^{\mathrm{grd,ISL}}_{pqrs}(\lambda,\Omega) = \int \frac{\partial^2 f}{\partial\nabla_\alpha s\partial\nabla_\beta s}u_\delta(\Omega)u_\omega(\Omega)\frac{\partial\nabla_\alpha m_\delta}{\partial D_{qp}}\frac{\partial\nabla_\beta m_\omega}{\partial D_{rs}}\mathrm{d}\boldsymbol{r}. \tag{19}$$

By noticing the identity $\langle u_\alpha(\Omega)u_\beta(\Omega)\rangle_\Omega = \frac{1}{3}\delta_{\alpha\beta}$, one reaches the final analytic expression of K^{grd}_{pqrs} in ISL treatment,

$$K^{\mathrm{grd,ISL}}_{pqrs} = \int \frac{1}{3}\frac{\partial^2 f}{\partial\nabla_\alpha s\partial\nabla_\beta s}\frac{\partial\nabla_\alpha m_\delta}{\partial D_{qp}}\frac{\partial\nabla_\beta m_\delta}{\partial D_{rs}}\mathrm{d}\boldsymbol{r}, \tag{20}$$

which is numerically stable and spin-rotation symmetry conserved. In summary, the noncollinear GGA kernel for closed-shell systems in the ISL approach reads

$$\begin{aligned} K^{\mathrm{ISL}}_{pqrs} = K^{\mathrm{nn}}_{pqrs} &+ \int \frac{\partial^2 f}{\partial s^2}\frac{\partial\boldsymbol{m}}{\partial D_{qp}}\cdot\frac{\partial\boldsymbol{m}}{\partial D_{rs}}\mathrm{d}\boldsymbol{r} \\ &+ \int \frac{\partial^2 f}{\partial s\partial\nabla s}\cdot\nabla\left(\frac{\partial\boldsymbol{m}}{\partial D_{qp}}\cdot\frac{\partial\boldsymbol{m}}{\partial D_{rs}}\right)\mathrm{d}\boldsymbol{r} \\ &+ \int \frac{1}{3}\frac{\partial^2 f}{\partial\nabla_\alpha s\partial\nabla_\beta s}\frac{\partial\nabla_\alpha m_\delta}{\partial D_{qp}}\frac{\partial\nabla_\beta m_\delta}{\partial D_{rs}}\mathrm{d}\boldsymbol{r}. \end{aligned} \tag{21}$$

Let us now turn to the comparison of existing formulations of noncollinear GGA kernels in closed-shell systems. Compared with the formulation proposed by Bast and co-workers, the only difference is the factor $\frac{1}{3}$ in the last term of Eq. (21). The formulation proposed by Bast and co-workers directly extending from the collinear GGA formulation has the correct collinear limit. However, K^{ISL}_{pqrs} derived directly from Eq. (18) may maintain more nature of the noncollinear GGA functional. Nevertheless, this advantage of ISL should not be overstated since different limit processes may lead to different results. Egidi and co-workers [11] proposed another formulation for GGA kernels, suggesting evaluating the scalar spin-density s in Eq. (5) as

$$s = \tfrac{1}{3}(m_x + m_y + m_z), \tag{22}$$

at girds with small $\boldsymbol{m}$ (like $|\boldsymbol{m}| < 10^{-12}$). Such a treatment slightly breaks the rotational symmetry but can be uniformly used for closed-shell and open-shell systems. Equation (17) hints that ISL can be used for open-shell systems. However, when $|\boldsymbol{m}|$ is very small but $|\boldsymbol{m}| \neq 0$, there is no correction from ISL; thus the ISL approach for noncollinear GGA kernels inherits the numerical instabilities from regular treatment and is not advocated for open-shell systems.

At the end of this section, we address why this particular proximity vector (13) is chosen. For a given Ω, $\boldsymbol{u}(\Omega)$ is constant in the spatial space, respecting the translation invariance of spatial space. In addition, different Ω values share the same weight, indicating that the spin-polarization directions, $\boldsymbol{u}(\Omega)$, are isotropically (spherically) distributed to preserve the spin-rotation symmetry. Other distributions can also be adopted, such as an ellipsoidal distribution. For simplicity, we only consider the case in which two principal semiaxes, along the x and y axis, approach zero. In this case, the proximity vector, the counterpart of Eq. (13), is

$$\boldsymbol{m}(\lambda) = \boldsymbol{m} + \lambda\boldsymbol{u}_z, \tag{23}$$

and the kernel, the counterpart of Eq. (20), is

$$K^{\mathrm{grd}}_{pqrs} = \int \frac{\partial^2 f}{\partial\nabla_\alpha s\partial\nabla_\beta s}\frac{\partial\nabla_\alpha m_z}{\partial D_{qp}}\frac{\partial\nabla_\beta m_z}{\partial D_{rs}}\mathrm{d}\boldsymbol{r}. \tag{24}$$

It is evident that the kernel (24) breaks the spin-rotation symmetry. Furthermore, the degeneracy of triplet excitation energies, in the absence of spin-orbit couplings, will be broken by the kernel (24).

III. NUMERICAL RESULTS AND DISCUSSION

A. Implementation and computational details

Kernels play an important role in the LR-TDDFT (linear-response time-dependent DFT) [12] and CPKS (coupled perturbed Kohn-Sham) [6] equation. In this work, we implement ISL kernels for both LR-TDDFT and CPKS in the BDF package [13]. To cover the spin-orbit couplings with high precision, a four-component relativistic framework [14] is adopted with the restricted kinetically balanced basis [15] used for the small component of four-component spinors.

TABLE I. Calculated excitation energies ($ns^2 \rightarrow ns^1np^1$) (in eV) of Zn, Cd, and Hg with different noncollinear kernels.

			Formulation by Bast *et al.*[a]			ISL			
Atom	Term symbol	LDA	BLYP	BP86	PBE	BLYP	BP86	PBE	Expt. [31]
Zn	$^3P_0$	4.33(4.32)	4.23(4.22)	4.03(4.02)	3.98(3.76)	4.26	4.08	3.81	4.01
	$^3P_1$	4.35(4.35)	4.25(4.25)	4.06(4.04)	4.00(3.78)	4.28	4.11	3.83	4.03
	$^3P_2$	4.41(4.40)	4.30(4.30)	4.11(4.09)	4.05(3.83)	4.33	4.16	3.88	4.08
	$^1P_1$	5.76(5.76)	5.59(5.61)	5.66(5.67)	5.58(5.58)	5.59	5.66	5.58	5.80
Cd	$^3P_0$	3.95(3.95)	3.86(3.85)	3.66(3.66)	3.64(3.47)	3.87	3.69	3.46	3.73
	$^3P_1$	4.02(4.02)	3.92(3.92)	3.73(3.73)	3.71(3.54)	3.93	3.76	3.53	3.80
	$^3P_2$	4.17(4.17)	4.06(4.06)	3.88(3.88)	3.85(3.69)	4.07	3.91	3.67	3.95
	$^1P_1$	5.34(5.34)	5.17(5.18)	5.21(5.22)	5.14(5.14)	5.17	5.21	5.14	5.42
Hg	$^3P_0$	4.87(4.87)	4.74(4.74)	4.63(4.63)	4.60(4.45)	4.74	4.65	4.44	4.67
	$^3P_1$	5.08(5.08)	4.94(4.94)	4.85(4.84)	4.81(4.66)	4.94	4.86	4.66	4.89
	$^3P_2$	5.66(5.67)	5.47(5.48)	5.41(5.42)	5.34(5.21)	5.46	5.42	5.19	5.46
	$^1P_1$	6.52(6.53)	6.29(6.30)	6.40(6.42)	6.33(6.32)	6.29	6.40	6.33	6.70
MAE[b]		0.16	0.02	−0.08	−0.13	0.03	−0.05	-0.25	
MRE(%)[c]		4.03	1.20	−1.41	-2.45	1.44	−0.85	-5.49	
ME[d]		0.33	−0.41	−0.30	−0.37	−0.41	−0.30	−0.37	

[a]The data outside the parentheses are the excitation energies calculated by the formulation proposed by Bast and collaborators implemented in this work. The data in parentheses are the results reported by Bast *et al.* [10].
[b]MAE: Mean absolute error.
[c]MRE: Mean relative error.
[d]ME: Maximum error.

The ISL kernel is implemented in the LR-TDDFT module in the BDF package to calculate excitation energies of closed-shell systems based on the work by Gao *et al.* [16,17]. Quadruple zeta all-electron 4 polarization Slater-type orbitals [18], further augmented in an even-tempered fashion for the convergence of excitation energies, are used.

The ISL kernel is implemented in the CPKS module, also in the BDF package, to calculate two magnetic properties, the nuclear magnetic resonance (NMR) shielding constant [19,20] and nuclear-spin rotation (NSR) coupling tensor [21,22], based on the work in Refs. [23] and [21]. In both NMR and NSR calculations, very large Gaussian-type orbitals, initially developed for rare gas atoms in the same periods [24], are used to guarantee the convergence of the basis set. In calculations of the NMR shielding constants, the uniform external magnetic field brings two additional complexities. The first one is the uncertainty of gauge origin, which can be handled by gauge-including atomic orbitals (GIAO) [25]. The second one is the dramatic changes in the relation between the large and the small components of four-component spinors, which can be efficiently described via the magnetically balanced basis set [14,26]. In this work, we adopt the external field-dependent unitary transformation [20] basis set, one of the magnetically balanced basis sets, further combined with the GIAO, as described in Ref. [23].

The geometry of the linear uranyl (VI) ion UO_2^{2+} is taken from Ref. [11] with a bond length of 1.708 angstrom. The bond lengths of HF to HI are 0.9169, 1.2746, 1.4145, and 1.6090 angstrom, respectively, taken from Ref. [21]. The bond

TABLE II. Calculated lowest excitation energies (in eV) of UO_2^{2+} with different noncollinear kernels.

Reported by Egidi *et al.*[a]		ISL				
BLYP	PBE	BLYP	BP86	PBE	CASPT2[b]	LR-CCSD[c]
1.22	1.18	1.46	1.44	1.42	2.38	2.83
1.40	1.37	1.58	1.57	1.56	2.49	2.85
1.83	1.76	2.07	2.03	2.01	2.51	2.96
2.06	2.00	2.26	2.23	2.21	2.77	3.13
2.15	2.11	2.34	2.32	2.31	3.15	3.45
2.41	2.37	2.49	2.50	2.51	3.26	3.60
2.42	2.45	2.52	2.52	2.52	3.61	4.01
2.46	2.50	2.53	2.53	2.55	3.88	4.30

[a]Corresponds to Eq. (22); see Ref. [11].
[b]CASPT2: Complete active space second-order perturbation theory; see Ref. [32].
[c]LR-CCSD: Linear-response coupled-cluster theory including single and double excitations; see Ref. [33].

TABLE III. Calculated isotropic NMR shielding constants (in p.p.m.) of H and X in HX with noncollinear kernels.

		Formulation by Bast *et al.* [10]			ISL			
Molecule	LDA	BLYP	BP86	PBE	BLYP	BP86	PBE	Expt.[a]
				Isotropic shielding constants of H				
HBr	35.10	37.51	36.59	36.49	36.91	36.03	36.07	34.64
HI	42.92	47.81	45.67	45.50	45.99	43.98	44.18	42.88
HAt	59.47	69.33	64.39	64.38	64.86	60.36	61.03	
MAR	0.25	3.90	2.37	2.23	2.69	1.24	1.37	
MRE(%)	0.71	9.90	6.08	5.72	6.90	3.28	3.58	
ME	0.46	4.93	2.79	2.62	3.11	1.39	1.43	
				Isotropic shielding constants of X				
HBr	2921.17	2865.99	2893.27	2903.62	2863.30	2890.42	2902.30	2961.03
HI	5784.06	5677.61	5734.03	5757.54	5667.24	5722.79	5753.94	5829.97
HAt	17550.98	17395.32	17533.63	17614.21	17332.57	17462.60	17614.19	
MAR	−42.88	−123.70	−81.85	−64.92	−130.23	−88.89	−67.38	
MRE(%)	−1.07	−2.91	−1.97	−1.59	−3.05	−2.11	−1.64	
ME	−45.91	−152.36	−95.94	−72.43	−162.73	−107.18	−76.03	

[a]Mapped from experimental NSR coupling constants [21].

length of HAt is 1.7485 angstrom, taken from Ref. [22]. In this work, three GGA functionals, BLYP [8,27,28], BP86 [8,29], and PBE [30], are chosen for numerical tests.

B. Excitation energy calculations

Table I lists the excitation energies ($ns^2 \rightarrow ns^1np^1$) of Zn, Cd, and Hg in ISL and the formulation proposed by Bast and co-workers. Excitation energies calculated by formulation proposed by Bast and co-workers reported in Ref. [10] and implemented in BDF are in good agreement, except for the PBE functional. However, our results for PBE functional coincide with the results in Ref [9], reported by Komorovsky *et al.*, hinting at the correctness of our implementation.

It is found that the ISL formulation and formulation proposed by Bast and co-workers are close in values, and the agreements between two formulations compared with experiments [31] depend on systems and functionals, but in general are similar. For instance, ISL affords results closer to the experiment for BP86, while the formulation proposed by Bast and co-workers affords closer results for BLYP. Nevertheless, both formulations can afford more reasonable results for these excited states than LDA.

The LR-TDDFT calculations of UO_2^{2+} are listed in Table II. For UO_2^{2+}, ISL provides comparable results with the formulation proposed by Egidi and co-workers [11]. All the excitation energies are underestimated compared with post-Hartree-Fock methods [32,33].

C. Second-order magnetic property calculations

Table III lists the isotropic shielding constants of hydrogen halides. The numerical results obtained by ISL and the for-

TABLE IV. Calculated NSR coupling constants (in atomic unit) of H and X at the equilibrium geometry with noncollinear kernels.

		Formulation by Bast *et al.* [10]			ISL			
Molecule	LDA	BLYP	BP86	PBE	BLYP	BP86	PBE	Expt.[a]
				NSR constants of H				
HF	−74.75	−77.38	−76.94	−76.87	−77.31	−76.86	−76.82	−72.188(24)
HCl	−43.00	−44.93	−44.16	−44.03	−44.64	−43.88	−43.83	−42.227(139)
HBr	−43.14	−47.55	−45.63	−45.46	−46.06	−44.23	−44.44	−41.00(31)
HI	−49.21	−57.68	−53.70	−53.43	−53.86	−50.15	−50.71	−48.19(22)
MAE	−1.63	−5.99	−4.21	−4.04	−4.57	−2.88	−3.05	
MRE(%)	3.18	12.32	8.47	8.12	9.23	5.59	5.96	
ME	−2.57	−9.49	−5.51	−5.24	−5.67	−4.67	−4.63	
				NSR constants of X				
HF	297.00	336.44	329.80	327.23	336.56	329.93	327.26	278.557(20)
HCl	53.92	60.53	57.60	56.60	60.58	57.65	56.62	51.299(52)
HBr	301.60	335.53	319.93	313.50	336.70	321.18	313.79	278.95(8)
HI	365.11	404.69	385.15	376.58	407.99	388.73	377.41	340.44(30)
MAE	17.09	46.99	35.81	31.16	48.15	37.06	31.46	
MRE(%)	6.77	19.48	14.63	12.70	19.86	15.04	12.80	
ME	24.67	64.25	51.24	48.67	67.55	51.37	48.70	

[a]Experimental values at the equilibrium geometry [21], and the experimental uncertainty is in parentheses.

mulation proposed by Bast and co-workers are close to each other and in good agreement with the experimental data.

Table IV lists the calculated NSR coupling constants of hydrogen halides. Similarly, compared with the experimental data, results obtained from both formulation proposed by Bast and co-workers and the ISL formulation are reasonable.

We also observed that for both NMR and NSR, ISL provides slightly better agreement with the experimental data for H atom but slightly worse for heavy atoms than the formulation proposed by Bast and co-workers. Generally, their agreements with the experimental data are at the same level. Unlike LR-TDDFT calculations for excitation energies where GGA functionals provide better results than LDA, in NMR shielding and NSR tensor calculations, the LDA functional displays better agreement with experimental data than GGA.

IV. SUMMARY

ISL, an approach for noncollinear GGA kernels in closed-shell systems, is proposed in this work. Numerical stability, rotational symmetry conserving, and numerical tests hint that ISL is a potential candidate in noncollinear calculations for closed-shell systems. However, ISL does not have the correct collinear limit. In addition, ISL cannot help the numerical instabilities in open-shell systems and is not recommended for open-shell systems.

ACKNOWLEDGMENTS

Y.X thanks Zhendong Li and Sihong Shao for valuable discussions. This work was supported by the National Natural Science Foundation of China (21473002).

[1] U. Von Barth and L. Hedin, J. Phys. C: Solid State Phys. **5**, 1629 (1972).
[2] R. M. Dreizler and E. K. Gross, *Density Functional Theory: An Approach to the Quantum Many-Body Problem* (Springer Science & Business Media, 2012).
[3] J. Kübler, K.-H. Höck, J. Sticht, and A. Williams, J. Phys. F: Met. Phys. **18**, 469 (1988).
[4] S. H. Vosko, L. Wilk, and M. Nusair, Can. J. Phys. **58**, 1200 (1980).
[5] F. Wang and T. Ziegler, J. Chem. Phys. **121**, 12191 (2004).
[6] S. Komorovský, M. Repisk´, O. L. Malkina, V. G. Malkin, I. Malkin Ondík, and M. Kaupp, J. Chem. Phys. **128**, 104101 (2008).
[7] J. P. Perdew, J. A. Chevary, S. H. Vosko, K. A. Jackson, M. R. Pederson, D. J. Singh, and C. Fiolhais, Phys. Rev. B **46**, 6671 (1992).
[8] A. D. Becke, Phys. Rev. A **38**, 3098 (1988).
[9] S. Komorovsky, P. J. Cherry, and M. Repisky, J. Chem. Phys. **151**, 184111 (2019).
[10] R. Bast, H. J. A. Jensen, and T. Saue, Int. J. Quantum Chem. **109**, 2091 (2009).
[11] F. Egidi, S. Sun, J. J. Goings, G. Scalmani, M. J. Frisch, and X. Li, J. Chem. Theory Comput. **13**, 2591 (2017).
[12] M. E. Casida, Time-dependent density functional response theory for molecules, in *Recent Advances in Density Functional Methods* (World Scientific, Singapore, 1995), pp. 155–192, https://www.worldscientific.com/doi/pdf/10.1142/9789812830586_0005.
[13] Y. Zhang, B. Suo, Z. Wang, N. Zhang, Z. Li, Y. Lei, W. Zou, J. Gao, D. Peng, Z. Pu *et al.*, J. Chem. Phys. **152**, 064113 (2020).
[14] L. Cheng, Y. Xiao, and W. Liu, J. Chem. Phys. **130**, 144102 (2009).
[15] R. E. Stanton and S. Havriliak, J. Chem. Phys. **81**, 1910 (1984).
[16] J. Gao, W. Liu, B. Song, and C. Liu, J. Chem. Phys. **121**, 6658 (2004).
[17] J. Gao, W. Zou, W. Liu, Y. Xiao, D. Peng, B. Song, and C. Liu, J. Chem. Phys. **123**, 054102 (2005).
[18] E. Van Lenthe and E. J. Baerends, J. Comput. Chem. **24**, 1142 (2003).
[19] T. B. Demissie, M. Jaszuński, E. Malkin, S. Komorovský, and K. Ruud, Mol. Phys. **113**, 1576 (2015).
[20] Y. Xiao, W. Liu, L. Cheng, and D. Peng, J. Chem. Phys. **126**, 214101 (2007).
[21] Y. Xiao, Y. Zhang, and W. Liu, J. Chem. Theory Comput. **10**, 600 (2014).
[22] S. Komorovsky, M. Repisky, E. Malkin, T. B. Demissie, and K. Ruud, J. Chem. Theory Comput. **11**, 3729 (2015).
[23] L. Cheng, Y. Xiao, and W. Liu, J. Chem. Phys. **131**, 244113 (2009).
[24] J. Vaara and P. Pyykkö, J. Chem. Phys. **118**, 2973 (2003).
[25] F. London, J. Phys. Radium **8**, 397 (1937).
[26] Y. Xiao, W. Liu, and J. Autschbach, Relativistic theories of nmr shielding, in *Handbook of Relativistic Quantum Chemistry*, edited by W. Liu (Springer, Berlin Heidelberg, 2014), pp. 1–33.
[27] B. Miehlich, A. Savin, H. Stoll, and H. Preuss, Chem. Phys. Lett. **157**, 200 (1989).
[28] A. D. Becke, J. Chem. Phys. **96**, 2155 (1992).
[29] J. P. Perdew, Phys. Rev. B **33**, 8822 (1986).
[30] J. P. Perdew, K. Burke, and M. Ernzerhof, Phys. Rev. Lett. **77**, 3865 (1996).
[31] J. E. Sansonetti, W. C. Martin, and S. L. Young, Handbook of basic atomic spectroscopic data, version 1.1, http://physics.nist.gov/handbook, NIST (2004).
[32] K. Pierloot and E. van Besien, J. Chem. Phys. **123**, 204309 (2005).
[33] F. Réal, V. Vallet, C. Marian, and U. Wahlgren, J. Chem. Phys. **127**, 214302 (2007).